RIDE-HAILING FARES AND DEMAND INTERACTIONS: INSIGHTS FROM MARKET ANALYSIS OVER SPACE AND TIME

Priyanka Paithankar
Department of Civil, Architectural, and Environmental Engineering
The University of Texas at Austin
301 E. Dean Keeton St, Austin, TX, 78712 priyanka.paithankar@utexas.edu

Kara M. Kockelman, Ph.D., P.E. (corresponding author)
Dewitt Greer Professor in Engineering
Department of Civil, Architectural, and Environmental Engineering
The University of Texas at Austin
301 E. Dean Keeton St, Stop C1761, Austin, TX, 78712
kkockelm@mail.utexas.edu

Krishna Murthy Gurumurthy, Ph.D.
Transportation and Power Systems Division
Argonne National Laboratory, Energy Systems Division
9700 S. Cass Avenue, Argonne, IL 60439 kgurumurthy@anl.gov

Submitted for presentation at Bridging Transportation Researchers conference, August 2025.

ABSTRACT

Ride-hailing providers like Uber, Lyft, and Didi compete daily in global markets, yet existing research has largely overlooked the dynamic interdependence between fares and demand across time, location, and service providers. This study addresses that gap by jointly estimating the simultaneous relationship between demand and per-mile fares for Uber and Lyft in New York City (NYC). A system of simultaneous equations is solved using instrumental variables that account for cross-equation correlation and endogeneity. The analysis leverages operator-specific fare data and served-trip demand every 10 minutes over a 15-day period across NYC's 260 taxi zones. Weather variables (precipitation, temperature, wind speed) are used as instrumental variables to identify exogenous shifts in demand. A multiway-clustered variance estimator reflects heteroskedasticity plus correlations across time and space, and multiway block bootstrapping captures cross-cluster correlations. Model estimates suggest that a one-standard-deviation (1 SD) rise in Uber's and Lyft's fares will lower their respective demands by 27% and 89%, a 1 SD rise in precipitation lowers demand by 17%, and a 1 SD rise in temperature and wind speed raises demand by 4.4% and 3.7%, respectively. The cross-equation effects suggest that a 1 SD rise in demand results in a 9% rise in Uber's per-mile fares but just 2.2% in Lyft's fares, suggesting far more surge protection under Lyft's pricing plans.

Keywords: ride-hailing services, market competition, supply and demand, TNCs, demand prediction, pricing strategies.

BACKGROUND

On-demand ride-hailing services are transforming urban travel patterns by facilitating efficient matching between drivers and passengers through smartphone apps (Wang et al., 2016; Chen et al., 2020; Ke et al., 2020; Zhou et al., 2022a and Zhou et al., 2022b). These apps collect real-time data from passengers and drivers, giving them control over short-term supply and demand. On the demand side, surge pricing, which varies based on time and location, influences passengers' choice of provider (e.g., Uber or Waymo rather than Lyft). On the supply side, providers adjust surge pricing and vehicle dispatching strategies to manage the availability of vehicles throughout the day (Chen et al., 2020). Ride-hailing apps are popular not just because of their convenience and technology but also due to their pricing strategies. To draw in more users, many of these apps give subsidies to both passengers and drivers (Wang et. al., 2016). It is also common for these operators to strategize their fares and services to capture a larger market share while competing in local markets. For instance, Didi and Uber China were in a price war until 2016, but by November 2023, Uber regained a portion of its lost market share, stabilizing competitive dynamics between the two companies. Didi also faces competition from Chinese rivals, like Shouqi, Meituan, and Shenzhou (Zhou et al., 2022a). Currently, Uber and Lyft compete in the U.S., while Grab and Gojek compete in Southeast Asia, Ola and Uber in India, Bolt and Uber in Europe, and Careem and Uber in the Middle East (Wang and Yang, 2019).

Most existing ride-hailing companies provide customers with choices between standard-sized economy vehicles (e.g., UberX and Lyft Line), premium vehicles (e.g., Lyft Lux and Uber Black), and extra seating options (e.g., UberXL and Lyft XL). However, many studies in the past (e.g., Paronda et al., 2016; Huang et al., 2023) have overlooked service type distinctions when modeling competition among ride-hailing operators. For instance, Paronda et al. (2016) analyzed Uber, conventional taxis, and GrabCar in the Philippines, finding that Uber's service was 75% faster than its competitors and 35% and 28% cheaper than GrabCar and taxis, respectively. Their findings also revealed that GrabCar was the most reliable for vehicle availability, while Uber received the highest service-quality ratings. But they did not consider the role of drivers as a third party in the competition and did not differentiate between the various ride options offered within each operator.

Some of these limitations were later addressed by Huang et al. (2023), who analyzed spatiotemporal variations in ride-hailing fares and driver behavior characteristics to assess the social welfare of passengers and drivers. They also evaluated market share and competition intensity to capture the competitive dynamics among four operators in New York City (NYC): Uber, Lyft, Juno, and Via. The results showed that competition was most intense during weekday morning rush hours (6 to 8 a.m.), significantly higher than on weekends. This study highlighted that greater competition intensity lowers passenger costs and raises driver income, although excessive competition reduces the profitability of ride-hailing operators. Similarly, Meskar et al. (2023) investigated spatiotemporal pricing, driver compensation, and matching rates on a dynamic fleet-based ride-hailing operator aimed at maximizing profits. Their study considered drivers' possibility to accept or decline ride requests and showed that networks with balanced demand patterns were the most profitable. They concluded that the more balanced the demand across the network, the higher the potential profit for the operator. But neither of these studies allowed for feedbacks between provider fares and (instantaneous) service demands.

A few studies have emphasized the effects of pricing dynamics on operator revenue in a competitive market (Chen et al., 2023; Huang 2023). Rather than directly using the intractable stochastic dynamic program to balance spatial–temporal mismatches between passenger demand and driver supply, Chen et al., 2023 proposed a deterministic convex program (DCP) that captures the trade-off between pricing revenue and vehicle availability across regions and time. Findings show that dynamic pricing adjusts to local shortages/surpluses when tested on NYC market and yielded 5–6% higher revenue and serves 3–4% more passengers versus a best-available static schedule. Huang (2023) focused more on fare strategy modelling using machine learning methods. He predicted NYC taxi fares using trip distance (computed via the Haversine formula) and passenger count, comparing linear regression, decision tree, and random forest models. As expected, all three achieve reasonably low error; the two tree-based methods gives more accurate results than ordinary least squares. The linear regression model yields an RMSE of 1.718, decision tree cuts that error by roughly 26% down to 1.277, and the random forest improves accuracy further with an RMSE of 1.264—an additional 1% improvement over the decision tree alone.

Fare-setting strategies under competition are not limited to ride-hailing markets. Airlines adjust fares to capture the market and optimize profits across millions of OD pairs and departure times. Paithankar et al. (2024) analyzed seasonality, cabin type, and other features affecting US-carrier airline fares using feasible generalized least square regression. They found that international trips from the U.S. between October and December are more expensive than those in June, and businessclass tickets cost nearly five times more expensive than economy-class tickets. While these studies shed light on pricing strategies, they fail to account for simultaneity between fares and demand levels, by day of year, departure time, and OD pair. In reality, fare adjustments influence demand, and demand fluctuations, in turn, affect fares, creating an endogeneity issue that requires a more robust estimation to capture these interdependencies effectively.

This simultaneity issue has been partially addressed by Parvez et al. (2023), who analyzed both the continuous decision of trip fare and the discrete destination choice of TNC users. They modeled fare with a linear regression (LR) whose right-hand side includes trip attributes (distance, peakperiod indicators, shared-ride flag), origin and destination activity measures (recent demand, distance to CBD), built-environment and weather covariates, plus a term for unobserved factors shared with destination choice. Destination choice is predicted by a multinomial logit (MNL) over 30 census-tract alternatives, with utilities that depend on origin–destination distance, land-use mix, infrastructure (bus stops, bike lanes, transit score), demographics, and the same latent factor in the LR. Their results show that the joint LR-MNL model outperforms separate fare and destination models: the joint system achieves a higher log-likelihood (LL = 222,717.00 vs. 222,857.92 for the independent models) and a lower Bayesian information criterion (BIC = 45,793.20 vs. 46,075.04). In the fare equation, trip distance is the strongest positive driver of cost, peak-period trips carry a significant surcharge, shared trips command lower fares, and both built-environment (e.g., distance from CBD, nearby transit stations) and weather (snow depth) show measurable influence on fares. In the destination choice model, longer OD distances and residential or institutional land uses suppress choice probability, while commercial/recreational areas, higher transit and walk scores, and street density attract more trips. All else equal, rides that begin farther from the central business district had higher fares, presumably due to drivers covering longer distances empty ("dead heading") to pick up riders located far from other trip-makers, resulting in more empty miles (as discussed in Gurumurthy et al., 2021, for example).

Related to this, Özkan (2020) derived structural insights into when simple “charge-everyone-thesame” fares and “serve-only-local” matches suffice, and when operators must instead tailor prices by origin and allow cross-zone matching to beat one-size-fits-all policies by embedding both pricing and matching decisions into one optimization, subject only to supply-demand flow conservation and the requirement that drivers earn the same per-unit-time revenue wherever they sit. He showed that, under realistic heterogeneity in willingness to pay, the joint “origin-based pricing + cross-matching” scheme can raise total match rates by up to 60% over price-only or match-only baselines—even when accounting for dead-heading costs—whereas in the special case of uniform valuations simple constant fares and local matching are already optimal.

Unlike Özkan (2020), Dey et al. (2021) did a data-driven, city-wide analysis of NYC’s taxi market by jointly modeling two linked phenomena: the total number of monthly trips originating (from January 2015 to December 2018) in each of the city’s 259 taxi zones, and the proportion of those trips served by Yellow taxis, Green taxis, or TNCs (Uber/Lyft/Juno/Via). They fit a joint econometric system made up of a negative-binomial count model for total trips and a multinomial fractional-split model for service shares, linked through shared latent-factor terms and estimated via simulated maximum likelihood using scrambled Halton sequences. Their results reveal that ride-hailing demand more than doubled over the study period—TNCs grew from 13% to 70% of all dispatches by late 2018—while traditional taxi volumes fell sharply. In the demand model, zones with higher job density, more zero-car households, and greater transit access saw the largest increases in trip counts, whereas snow depth and dense bike-lane networks depressed ride-hailing use. In the share model, higher population and median-income areas tended to favor yellow taxis, while zones farther from airports and with lower transit access shifted toward TNCs; zero-car households also raised both Green-taxi and TNC shares. A positive correlation term confirms that unobserved factors boosting the Yellow-taxi share also tend to boost the TNC share.

Although most prior studies overlook distinctions by vehicle type, a few have examined servicespecific attributes and pricing. Schwieterman (2019) conducts a paired-trip analysis of Lyft, Lyft Line, UberX, UberPool, and Chicago Transit Authority (CTA) services in Chicago and finds that ride-hailing fares cost between \$42 and \$108 per hour of travel-time saved—far above the \$14.95 per hour value of time for personal travel recommended by the U.S. DOT (UDOT 2016, in 2018 dollars). Nevertheless, for business travelers—who the same guidance values at \$28.85 per hour— and for trips between neighborhoods poorly served by transit, ride-hailing often remains a costeffective alternative. Meanwhile, Chao (2019) took a more focused approach and analyzed UberX’s surge pricing, which adjusts fares in real-time based on demand, supply, and other external conditions. He used real-time operational data from Uber's APIs for ten different origindestination pairs, and controlled for weather (thunderstorms, squalls, mist/clouds), time of day, and day of the week. However, Schweiterman (2019) and Chao (2019) did not control for or discuss competition between providers. This gap is important to address, since competition can dramatically affect total demand, mode splits, provider profits, and traveler welfare. Demand fluctuates across time and space, as a function of trip type, land uses, traveler wealth, impatience, and so on. For example, passengers from higher-income residential areas are more willing to pay for shorter wait times and more luxurious vehicles. As a result, competition may vary greatly across different parts of a city and region, depending on the availability and popularity of ridehailing services by neighborhood and time of year.

Several studies highlight demographic and built environment impacts on taxi demand (and, to some extent, supply). McNally and Rafiq (2021) identified population and employment as key factors, while Qian and Ukkusuri (2015) linked lower income neighborhoods to fewer NYC taxi trips. Yu & Peng (2019) emphasized the effects of the built environment on ride-sourcing. Spatial imbalances dominate taxi demand, with 90% of trips concentrated in Manhattan (Qian and Ukkusuri, 2015), district-level disparities in Munich (Jager et al., 2016), and local imbalances in Shanghai (Liu et al., 2012). Geographically Weighted Regression (GWR) models (Chen et al., 2021; Li et al., 2019) address spatial heterogeneity; however, spatial spillover effects, or interactions between neighboring areas, remain underexplored. While studies including Correa et al. (2017), Pan et al. (2019), and Lavieri et al. (2018) employed spatial error/lag models or multivariate count models, none fully address spatial autocorrelation in explanatory variables or quantify spillover effects. Temporally, demand fluctuates daily (Zhu and Mo, 2022; Liu et al., 2015) and weekly (Zhao et al., 2016), with time series (Moreira-Matias et al., 2013) and machine learning (Zhou et al., 2019a) aiding prediction. This study bridges existing gaps by jointly estimating ride-hailing demand and corresponding fares while accounting for spatial and temporal spillover effects.

This gap is important to address for dense urban areas like NYC, where competition among ridehailing operators is influenced not only by spatiotemporal variations but also by regulatory policies and consumer preferences. In January 2025, the New York State government started a $1.50 congestion charge to be added to Uber and Lyft fares for trips entering Manhattan south of East 60th Street, which is passed on to riders (Congestion Pricing Program 2024). This charge is in addition to the existing For-Hire Vehicle Congestion Surcharge of $2.75, which applies to all ridehailing trips that both begin and end in New York State and either begin, end, or pass-through Manhattan south of, but not including, 96th Street (Congestion Surcharge, 2024). These fare updates have influenced the demand for Manhattan ride-hailed trips, and probably also their fares, as consumers may shift among service options available to reduce costs or avoid premium services. This dynamic disequilibrium affects the competitiveness and pricing strategies of ride-hailing providers, and this study examines the interdependence between fare and demand across NYC operators.

This study extends previous research (Zheng et al., 2022; Zhu et al., 2022) by modeling competitive fare interactions between two dominant ride-hailing operators while incorporating spatiotemporal spillover effects that influence pricing strategies across urban regions and endogeneity between fare and demand. It advances the understanding of fare and demand variation among ride-hailing operators using a three-stage least square (IV3SLS) estimation approach to analyze Uber and Lyft trips in NYC. It sheds light on how fare strategies diverge across operators, neighborhoods, and times of day by integrating trip data with demographic, weather, and built environment variables. The following section outlines the datasets used in this study, followed by a description of the methodology employed. The last two sections present model estimates, and a summary of findings.

DATA DESCRIPTION

This paper leverages detailed ride-hailing trip data from NYC (TLC Trip Record Data, 2023) across all five boroughs (Bronx, Brooklyn, Manhattan, Queens, and Staten Island) and Newark Airport. The full dataset includes trip records from medallion-regulated yellow and green taxis alongside app-based for-hire services; however, our analysis is confined to the Uber and Lyft subsets, comprising approximately 9.8 million rides between September 15 and September 30, 2024. These trips represent roughly 65–70% of the total for-hire vehicle market in New York City (NYC TLC, 2024). The variations of 2024 ride-hailing volumes over a year reveal a gradual upward trend in average daily trips for Uber and Lyft, rising from about 630,000 in January 2024 to approximately 680,000 in December 2024. Seasonal demand intensifies during the October–December window, likely driven by holiday travel and year-end social activity. The highest daily average observed since January 2021 occurred in March 2024, peaking near 690,000 trips per day. September was selected as a reference period because it reflects normative urban mobility conditions—schools are fully in session, workplaces operate at normal capacity, COVID-19 impacts have significantly diminished, and extreme weather conditions are generally absent.

TLC Trip Record Data show pickup (trip start) and end times (to the second), origins and destinations (to the level of 260 taxi zones), network distance traveled per trip (in tenths of miles), whether the ride was requested as a shared ride, and whether a match was made. It includes details on the base fare and any additional fees, such as, tolls, surcharges, and airport fees. These zones collectively span over 306 square miles, covering the primary regions Uber and Lyft serve. Queens is the largest borough, covering approximately 112 square miles, followed by Brooklyn (68.1 sq mi), Staten Island (58.2 sq mi), and the Bronx (42.6 sq mi). Manhattan covers 22.7 square miles, reflecting its dense urban environment and high trip demand. The dataset also includes the EWR zone (Newark Airport) as a destination but not as an origin, just 2.84 square miles, capturing intercity trips and airport-related travel. Zone sizes vary considerably, with Queens having the largest average size (1.62 sq mi per zone) and Manhattan having the smallest (0.33 sq mi per zone).

Manhattan dominates ride hailing demand (and supply), with 40.8% of all pickups and 37% of all drop-offs, reflecting its very high population and jobs densities and major tourist attractions (e.g., Broadway Theater district, Central Park, Museum of Modern Art, Brooklyn Heights and Prospect Park West). Brooklyn follows with 25.6% of pickups and 25.5% of drop-offs and Queens accounts for 20.6% of pickups and 20.3% of drop-offs, which aligns with its residential nature and proximity to major airports (JFK and LaGuardia airport). The Bronx contributes 11.5% of pickups and 10.9% of drop-offs, and Staten Island has just 1.40% of pickups and 1.38% of drop-offs, thanks to much lower densities, high parking supply, and heavy reliance on personal vehicles. While the Newark Airport contributes nearly zero pickups (0.00001%), it accounts for 0.70% of drop-offs. The remaining 4% of drop-offs show as "unknown" zone, suggesting that those originated outside NYC's mapped taxi zones (e.g., long-distance trips from New Jersey, Connecticut, and upstate New York).

Table 1 provides summary statistics of all variables available in this dataset. Uber dominates NYC's ride-hailing market, with approximately 72% of all trips analyzed (compared to Lyft's 28%). The ride-sharing requests are relatively low, with only about 3.07% of all trips involving riders requesting this service and an even smaller fraction (0.99%) resulting in a matched ride. Approximately 41% of trips incurred a congestion surcharge ($2.75 per trip), indicating that these rides began and ended in New York State and either originated, concluded, or passed through Manhattan south of 96th Street, while 24% of trips either originated, concluded, or passed through new congestion zone, which extends from 60th Street down to Battery Park and will now pay additional $1.5 per trip as per NYC's congestion pricing program launched on January 5, 2025

(NYC TLC, 2024). In addition to these congestion fees, riders are subject to a $2.50 Airport Fee for airport-related trips, an 8.875% sales tax, and a 2.75% Black Car fund fee, which contributes to driver benefits and safety programs (Lyft Blog, 2025).

TABLE 1 Summary Statistics of NYC's Uber + Lyft Trips from September 15 to 30, 2025
(n = 9,875,667 ride-hailed trips)

Variable Name	Mean	Std. Dev	Min	Median (50%)	Max
Trip Distance (miles)	2.87 mi	5.93	0.00	2.21	10.9
Trip Duration (minutes)	18.4 min	10.98	0.00	15.8	52.1
Passenger Wait Time per Trip (min)	4.66 min	2.24	0.00	4.25	11.3
Fare Paid per Trip ($)	$16.19	7.32	0.00	14.5	43.6
Fare per mile-Uber ($ per mile)	$6.35	2.60	0.03	6.10	15.6
Fare per mile- Lyft ($ per mile)	$8.07	3.03	0.01	6.50	15.6
Tolls Paid per Trip ($)	$0.72	2.65	0.00	0.00	66.6
Black Car Fund per Trip ($)	$0.46	0.22	0.00	0.42	1.16
Sales per Tax per Trip ($)	$1.43	0.65	0.00	1.28	3.43
Congestion Surcharge per Trip ($)	$0.93	1.30	0.00	0.00	5.50
Airport Fee per Trip ($)	$0.19	0.67	0.00	0.00	7.50
Tips Paid per Trip ($)	$1.01	2.72	0.00	0.00	100
Driver's Pay per Trip ($)	$13.7	6.18	0.00	11.3	30.9
Monday Trips (Indicator)	0.12	0.32	0.00	00.0	1.00
Tuesday Trips (Indicator)	0.12	0.32	0	0	1.00
Wednesday Trips (Indicator)	0.12	0.33	0	0	1.00
Thursday Trips (Indicator)	0.13	0.34	0	0	1.00
Friday Trips (Indicator)	0.21	0.41	0	0	1.00
Saturday Trips (Indicator)	0.17	0.37	0	0	1.00
Sunday Trips (Indicator)	0.14	0.34	0	0	1.00

The spatial distribution of ride pickups and drop-offs across various taxi zones (Figure 1) reveals distinct patterns of ride-hailing activity across NYC. Figure 1a shows a higher average number of daily pickups, with Central and Lower Manhattan experiencing the most activity. Areas in Brooklyn and Queens, particularly those near major transportation hubs or densely populated neighborhoods, also show higher pickup activity, although to a lesser extent than central Manhattan. The distribution of drop-off activity, as shown in Figure 1b, closely mirrors the pickup patterns, with central and lower Manhattan emerging as the primary hotspots, indicating Manhattan as a key destination for work, entertainment, and tourism. The major airports, such as, John F. Kennedy International Airport (JFK), experienced a high volume of pickups and drop-offs, while the Bronx and Staten Island showed significantly lower demand. Figure 2 shows distinct contrasts in the weekday and weekend pickup patterns in NYC. On weekdays (Monday to Thursday), there are two pronounced peaks: one during the morning rush hour (7 am to 9 am) and another during the evening rush hour (4 pm to 8 pm).

These peaks correspond to the commuting patterns of individuals traveling to and from work or school, indicating that ride-hailing services are heavily used for daily commuting during these times. On Fridays, evening pickup activity remains elevated well beyond traditional commuting hours, extending into the late-night period as people transition from work-related travel to social and entertainment-related trips. The sharp increase in pickups on Friday mornings suggests a potential spillover effect from late Thursday night activities, leading to sustained demand in the early hours of Friday. Saturdays experience the highest ride-hailing demand during the late evening and night, peaking between 9 pm and 2 am, a trend likely driven by nightlife and leisure activities. Unlike weekdays, weekend mornings typically see lower pickup counts, especially between 5 am and 9 am. This difference suggests that while weekdays are characterized by structured, commute-based travel, weekends see more varied and socially driven ride-hailing usage. Newark Airport, located in New Jersey, is not part of NYC, so very few pickup rides are recorded from that zone, as shown in Figure 1a. However, many trips originating in NYC end at Newark Airport, with 69,437 drop-offs recorded (i.e., 0.7% of NYC TNC drop-offs during the first half of September 2023).

Meanwhile, LaGuardia Airport and JFK Airport zones reported the highest share of pickups (3.8%) and drop-offs (4.5%), as shown in Figure 1. Figure 3 illustrates the temporal variation in the average fare per mile for ride-hailing trips across days of the week and hours of the day. Figures 3a and 3b show a clear trend where average fares peak during commuting hours, particularly in the late afternoon and early evening on weekdays, corresponding to the typical evening rush hours. This is especially pronounced on Wednesdays and Thursdays, where average fares per mile exceed $7 during peak hours, highlighting increased demand and potentially limited supply during these timeframes. In contrast, fares are generally lower during early morning hours (midnight to 5 AM) and late at night, reflecting reduced demand during off-peak periods. Interestingly, the weekends display a different pattern compared to weekdays. While fares remain moderate during the daytime, there is a noticeable rise in the early evening, likely due to social and recreational activities that drive demand for ride-hailing services.

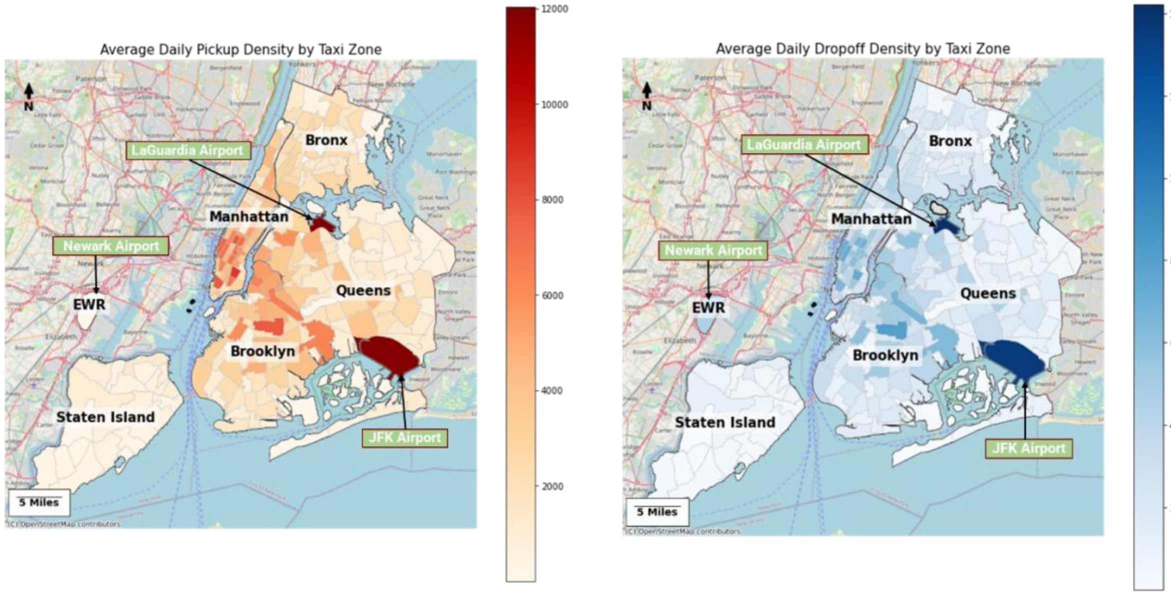

(a) (b) Figure 1 Daily Average Number of Pickups (a) and Drop-offs (b) by Taxi Zone from September 15 to 30, 2025 (N=9,875,667 trips)

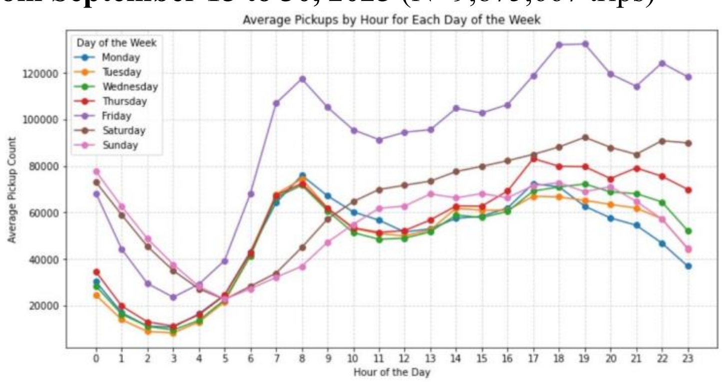

Figure 2 Daily Average Number of Pickups by Hour and Day of Week from September 15 to 30, 2025 (N=9,875,667 trips)

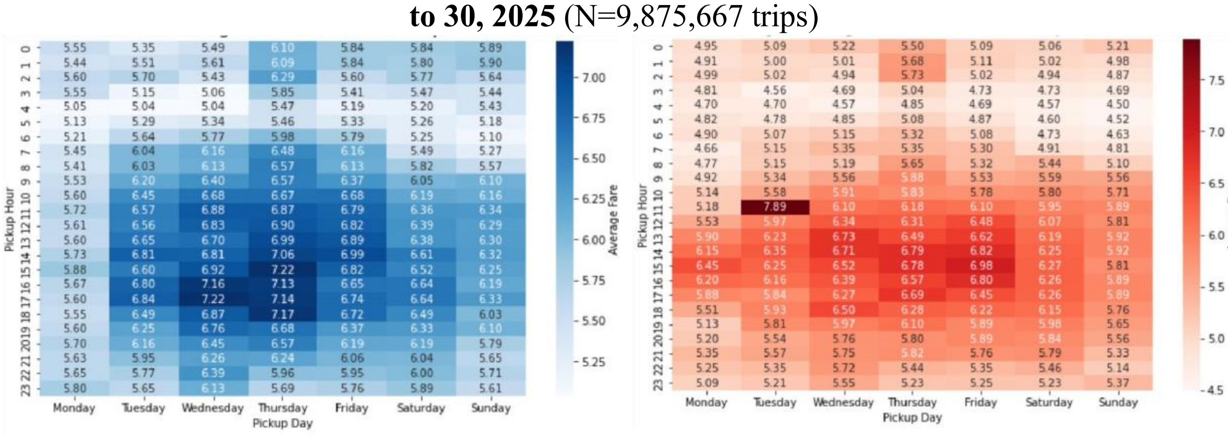

(a) (b) Figure 3 Temporal Variation in Average Fare per Mile Across Week and Time of the Day (N=9,875,667 trips)

The demographic data for the OD zones were obtained from EPA's Smart Location Data (NYC Planning, 2024). In a competitive ride-hailing market, fare, destination, and trip distance all affect demand (i.e., the number of ride requests), and demand can also influence fares. Daily weather conditions were included in the analysis by retrieving daily meteorological data from Meteostat (2023), at the weather station nearest Manhattan (40.7128° N, –74.0060° W). This data includes average temperature, total precipitation, and average wind speed for each calendar day. These variables were then merged with the ride-hailing records by date, ensuring that each 10-minute fare bin in a given zone was associated with the corresponding daily weather conditions. During peak periods, a surge in trip requests might lead to surge pricing, which raises fares. This surge in demand may also lead to congestion, resulting in longer trip durations. To analyze the interdependence between demand, supply, and fares, trips were grouped into 10-minute bins (over 15 days and 24 hours) for each of the 260 zones, capturing short-term demand fluctuations. Of a potential 561,600 bins (260 zones × 15 days × 24 hours × 6 bins per hour), 495,128 bins exist in the dataset.

TABLE 2 Summary Statistics of Trip, Demographic, Built-Environment, and Weather Variables Within Spatiotemporal Bins (N = 495,128)

	Mean	Median	Std Dev	Min	Max
Demand (Trips Served within bin)	308.4	239.5	253.8	2.0	2064
Uber's Fare ($ per mile within bin)	6.24	6.19	1.09	2.70	11.84
Lyft's Fare ($ per mile within bin in zone)	6.09	5.65	2.42	0.09	13.68
Population density (people/acre in zone)	52.71	9.73	94.4	0.0	728.1
Employment density (jobs/acre in zone)	106.9	3.53	475.1	0.0	4925
Household workers per job in zone (workers/job in zone)	0.501	0.121	0.678	0.0	3.39
Total road network density (facility miles of road links per square mile in zone)	35.87	26.07	49.07	0.0	355.5
Street intersection density (intersections per square mile in zone)	182.7	72.9	278.9	0.0	1804
Gross population density (people/acre) at Pickup Zone	54.65	14.1	95.9	0.0	728.1
Gross employment density (jobs/acre) at Pickup Zone	111.59	3.69	486.6	0.0	4925
Count of workers earning $1250 per month or less at Pickup Zone	185.8	115.8	288.2	0.0	2407
Count of workers earning between $1250 to $3333 per month at Pickup Zone	275.7	147	456.7	0.0	4052
Count of workers earning $3333 per month or more at Pickup Zone	416.6	196	668.6	0.0	5398
Number of Jobs in Zone per Household in Pickup Zone	33.6	0.22	256.9	0.0	3034
Number of Household Workers per Job at Pickup Zone	0.49	0.12	0.68	0.0	3.40
College/Associate Degree Graduate people per Capita (Pickup Zone)	0.13	0.14	0.05	0.0	0.24
Bachelor’s Degree Graduate people per Capita (Pickup Zone)	0.16	0.15	0.09	0.0	0.48
Professional Degree Graduate people per Capita (Pickup Zone)	0.13	0.09	0.1	0.0	0.40
Married (Except Separated) people per Capita (Pickup Zone)	0.31	0.31	0.10	0.0	0.49

Divorced or Separated people per Capita (Pickup Zone)	0.08	0.08	0.03	0.0	0.15
Widowed people per Capita (Pickup Zone)	0.04	0.04	0.02	0.0	0.13
Daily Average Precipitation (mm)	0.307	0.00	3.41	0.0	78.9
Daily Average Temperature (°C)	19.37	19.0	1.07	16.1	23.0
Daily Average wind speed (mi/h)	9.204	9.20	0.94	6.7	28.5
UN General Assembly Meeting (September 19–23, 2025)	0.009	0.00	0.09	0.0	1.00
Climate Week (September 17–24, 2025)	0.032	0.00	0.18	0.0	1.00
Global Citizen Festival (September 23, 2025)	0.001	0.00	0.031	0.0	1.00
New York Film Festival (September 29 – October 15, 2025)	0.001	0.00	0.031	0.0	1.00

METHODOLOGY

In this competitive ride-hailing market, endogeneity arises because demand (in terms of total trips) and fares (for both Uber and Lyft) are determined simultaneously—i.e., demand depends on fares, while fares adjust in response to demand. Such simultaneity renders the ordinary least squares estimators inconsistent if the error terms are correlated with the endogenous regressors. Thus, each fare equation (Eq 2 and 3) contains demand as a right-hand-side variable, yet demand is itself a function of those fares. To resolve this feedback correlation, instrumental variables are employed within a 3SLS framework (Zha et al., 2017; Feng et al., 2023). Weather variables (precipitation, temperature, and wind speed) are expected to shift demand but not directly enter the fare-setting equations (apart from their effect on demand), so they are used here as instrumental variables. By instrumenting demand in each fare equation with exogenous weather shocks, the model specification seeks to ensure that the fare regressions capture the causal effect of demand on fares, free from the reverse causal feedback.

The 3SLS estimator then jointly estimates three equations: for demand (Eq. 1), Uber's per-mile fare (Eq. 2), and Lyft's per-mile fare (Eq. 3), while allowing for correlation among the error terms. This approach mitigates bias from simultaneity and yields consistent parameter estimates. In practice, the error terms in these equations are correlated within a particular location over time (temporal autocorrelation) or across nearby locations on the same date (spatial autocorrelation). To address these dependencies (Tang et al., 2019; Oh et al., 2020; Wang et al., 2022), this study allows for clustered and heteroskedastic standard errors. across timestamps and zones (He at al., 2019; Kelleney and Ishak, 2021; Xing et al., 2022; Zhu et al., 2023; Zhang et al., 2023). The analysis uses trip counts summed and trip fares-per-mile averaged over 10-minute intervals by zone and operator.

$$QQ_{iiiiTTTTiiTTTT} = \beta\beta_0 + \beta\beta_1 WW_{iiii} + \beta\beta_2{}^{FF}{}_{iiiiUU} + \beta\beta_3{}^{FF}{}_{iiiiLL,rrrrrr} + \quad \gamma\gamma_{jj}{}^{XX}{}_{iiEEEEEEjj}$$

$$+\ \delta\delta_{kk}{}^{XX}{}_{iiEEEEEEkk} \qquad {}_{,MMTTrriiiiTTTT\ rriiTTiiEErr} \quad {}_{jj} \quad {}_{kk}$$

$$+\ \theta\theta_{mm} XX_{ii\text{Weather}} + uu_{iiii} \ldots \ldots \ldots \ldots \ldots \ldots \ldots \ldots \text{(Eq. 1)} \quad {}_{mm}$$

$FF_{iiiiUU} = \alpha\alpha0 + \alpha\alpha1 QQ_{iiii\text{total}} + \alpha\alpha2 WW_{iiii} + \phi\phi_{mm} XX_{ii\text{FareEPA}\, mm} + \psi\psi_{nn} XX_{ii\text{Edu,}}$ Maritalnn Status $+ \rho\rho_{pp} DD_{ii\text{Events}}$

mm nn pp

$+ vv_{iiii}$ … … … … … … … … (Eq. 2)

$FF_{iiiiLL} = \delta\delta0 + \delta\delta1 QQ_{iiii\text{total}} + \delta\delta2 WW_{iiii} + \lambda\lambda_{qq} XX_{ii\text{FareEPA}qq} + \mu\mu_{rr} XX_{ii\text{Edu,Marital}rr}$ Status $+ \eta\eta_{rr} DD_{ii\text{Events}}$

qq rr rr

$+ ww_{iiii}$ … … … … … … … … (Eq. 3)

The demand equation models the total number of trips ($QQ_{iiii}{}^{TTTTiiTTTT}$) in a pickup zone ii and during a10-

minute time interval tt. This demand is influenced by several factors, including passenger wait times, fares, socioeconomic characteristics, and weather conditions. $\beta\beta_1 WW_{iiii}$ represents the effect of wait times (WW_{iiii}) on demand. The coefficients $\beta\beta_2$ and $\beta\beta_3$ correspond to the effects of Uber fares $FF_{iiii}{}^{UU}$ and Lyft fare residuals ($FF_{iiii}{}^{LL,\text{res}}$), respectively. The equation also includes EPA demographic variables $\sum_{jj} \gamma\gamma_{jj}\, XX_{ii}{}^{EEEEEE}{}_{jj}$, which represent pickup-zone attributes, like education levels, employment rates and household incomes. These variables help explain how socioeconomic factors in a pickup zone affect ride-sharing demand. Similarly, education and marital status variables

($\sum_{kk} \delta\delta_{kk}\, XX_{ii}{}^{EEEEEE}{}_{kk}{}^{,MMTTrriiiiTTTT}$) capture demographic influences on demand. The weather variables $\sum_{mm} \theta\theta_{mm} XX_{ii}{}^{WWrrTTiihrrrr}$ such as, precipitation, average temperature, and wind speed, are included to account for temporal variations in demand caused by weather conditions. The error term (uu_{iiii}) captures unobserved factors that affect demand which may include sudden events or localized disruptions not explicitly specified in the model.

The Uber fare equation (Eq 2) models the average Uber fare per mile $FF_{iiii}{}^{UU}$ in a pickup zone ii during a 10-minute time interval tt., as a function of demand, wait times, socioeconomic characteristics (of pickup zone residents), and event-specific shocks. The constant term ($\alpha\alpha_0$) represents the baseline Uber fare when all other variables are zero. The term $\alpha\alpha_1 QQ_{iiii}{}^{\text{total}}$ captures the relationship between total trip demand ($QQ_{iiii}{}^{\text{total}}$) and Uber fares. Higher demand typically leads to increased fares to balance demand and supply. The term $\alpha\alpha_2 WW_{iiii}$ accounts for the effect of wait times (WW_{iiii}), with longer passenger wait times potentially indicating lower ride availability, which could drive up fares. The model aggregates neighborhood-specific socioeconomic factors

($\sum_{mm} \phi\phi_{mm} XX_{ii}{}^{\text{FareEPA}}{}_{mm}$)—capturing employment and income levels—along with normalized education and marital status variables $\sum_{nn} \psi\psi_{nn} XX_{ii}{}^{\text{Edu}}{}_{nn}{}^{,\ \text{Marital}}$). For example, areas with higher proportions of certain demographic groups might exhibit different ride-sharing pricing patterns.

Lyft's fare equation (Eq 3) similarly follows a similar structure, incorporating real-time supply constraints (via wait times WW_{iiii}), local demand ($QQ_{iiii}{}^{\text{total}}$), and economic, demographic factors ($\sum_{qq} \lambda\lambda_{qq} XX_{ii\text{FareEPA}qq}$, $\sum_{rr} \mu\mu_{rr} XX_{iiEEEEEErr}$ $_{,MMTTrriiiiTTTT}$). Event indicator variables ($\sum_{pp} \rho\rho_{pp} DD_{ii\text{Events}}$, $\sum_{rr} \eta\eta_{rr} DD_{ii\text{Events}}$) capture temporal shocks for both Uber and Lyft, respectively, events like conferences or festivals that can increase demand and lead to higher fares. The error term vv_{iiii} and ww_{iiii} account for unobserved local factors that influence each operator's fares in pickup zone ii at time interval tt. he variance-covariance of the errors, Var$\varepsilon\varepsilon_{ii,ii}$, not assumed to be independent and identically distributed. Instead, Var$\varepsilon\varepsilon_{ii,ii}$ $= \Omega$ allows within-cluster correlation. For example, if errors are clustered by pickup zone ii means all observations in the location ii across different times tt may have correlated errors and observations in different locations $ii \neq jj$ are taken to be uncorrelated. In this analysis, errors are clustered by a combined identifier that merges the location and timestamp, so that all observations sharing the same cluster CC (ii, tt) can show correlated errors. The clusterrobust estimator of the variance-covariance matrix for $\beta\beta\hat{}$ is then defined as follows:

$$\text{Var}\ (\beta\beta\hat{})_{\text{cluster}} = (\text{X}'\text{X})^{-1} \sum_{cc=1}^{CC} \text{X}_{cc}{}'\, \varepsilon\varepsilon\hat{}_{cc}\, \varepsilon\varepsilon\hat{}_{cc}{}'\text{X}_{cc}\ (\text{X}'\text{X})^{-1} \dots\dots\dots\dots\dots\dots\dots\dots \text{(Eq. 4)}$$

Where, $cc = 1, \dots, CC$ indexes the clusters, X_{cc} is the design matrix for observations in cluster cc and

$\varepsilon\varepsilon\hat{}_{cc}$ represents the vector of residuals for that cluster. In system of equations, let ww_{iiii} , vv_{iiii} , uu_{iiii} denote the unobserved error terms in the demand, Uber fare, and Lyft fare equations, respectively, for location ii at time tt. These error components are then stacked into a single vector as follows;

$$\varepsilon\varepsilon_{ii,ii} = \begin{matrix} ww_{iiii} \\ vv_{iiii} \\ uu_{iiii} \end{matrix}$$

If $\varepsilon\varepsilon_{ii,ii}$ follows a multivariate distribution with a covariance matrix Σ, then cross-equation correlation arises whenever Σ is not diagonal. For instance, in a three-equation system, the covariance matrix (Σ, Eq. 5) allows for nonzero off-diagonal elements, indicating correlation across the demand ($QQ_{iiii}{}^{TTTTiiTTTT}$), Uber fare ($FF_{iiii}{}^{UU}$), and Lyft fare ($FF_{iiii}{}^{LL}$) equations.

$$\Sigma = \begin{matrix} \sigma\sigma_{DDDD} & \sigma\sigma_{DDUU} & \sigma\sigma_{DDLL} \\ \sigma\sigma_{UUDD} & \sigma\sigma_{UUUU} & \sigma\sigma_{UULL} \\ \sigma\sigma_{LLDD} & \sigma\sigma_{LLUU} & \sigma\sigma_{LLLL} \end{matrix} \dots\dots\dots\dots\dots\dots\dots\dots \text{(Eq. 5)}$$

Where, $\sigma\sigma_{DDUU} = \text{Cov}(ww_{iiii}, vv_{iiii})$, $\sigma\sigma_{DDLL} = \text{Cov}(ww_{iiii}, uu_{iiii})$, $\sigma\sigma_{UULL} = \text{Cov}(vv_{iiii}, uu_{iiii})$. The diagonal elements

$\sigma\sigma_{DDDD}$, $\sigma\sigma_{DDDD}$, $\sigma\sigma_{DDDD}$ represent the variances of the errors in each equation, and the off-diagonal elements $\sigma\sigma_{DDUU}$, $\sigma\sigma_{DDLL}$, $\sigma\sigma_{UULL}$ capture the covariance between pairs of error terms. For instance, $\sigma\sigma_{DDUU}$ measures the correlation between the demand and Uber fare equation errors.

While robust variance estimator addresses heteroskedasticity within each cluster, it does not account for cross-cluster correlations. Citywide events or regional weather patterns can induce dependencies across these clusters. For instance, shocks affecting one zone might also impact neighbouring zones or different time intervals, creating cross-cluster correlations. Hence, this study employed the multiway cluster bootstrap method, which produces a distribution of bootstrap estimates for each model parameter and captures the variability across clusters. The multiway cluster bootstrap identifies the unique clusters in both the temporal ($\mathcal{TT}$) and spatial dimensions ($\mathcal{ZZ}$) and estimate the initial 3SLS model ($\theta\theta^{\hat{}}$) using the full dataset—serving as a point of reference for the bootstrap replications. In each bootstrap iteration (bb), clusters are resampled with replacement separately in each dimension, randomly drawing sample of fare bins (NN_{TT}) and zones (NN_{ZZ}), each of the same size as their original sets.

$$\mathcal{TT}_b^{*} = \{t^*_{b,1}, t^*_{b,2}, \dots , tt_{bb*,NNTT}$$

$$\mathcal{ZZ}_b^{*} = \{z^*_{b,1}, z^*_{b,2}, \dots , zz_{bb*,NNZZ}$$

Where, $\mathcal{TT} = tt_1, tt_2, \dots , tt_{NNTT}$ denote the set of time clusters (i.e., fare bins) and $\mathcal{ZZ} = zz_1, zz_2, \dots , zz_{NNZZ}$ denote the set of spatial clusters (i.e., zones), where NN_{TT} and NN_{ZZ} are the number of fare bins and zones, respectively. Let, $\theta\theta^{\hat{}} = \theta\theta^{\hat{}}_1, \theta\theta^{\hat{}}_2, \dots , \theta\theta^{\hat{}}_{pp}$ be the initial 3SLS parameter vector, with pp representing the number of estimated parameters, and let $bb = 1,2, \dots , BB$ denote bootstrap iterations. The bootstrap sample ($\mathcal{SS}_{bb}$, $EEEE$. 6) is then constructed by retaining only those observations ii whose fare bin belongs to $\mathcal{TT}_{bb^*}$ and whose zone belongs to $\mathcal{ZZ}_{bb^*}$.

$$\mathcal{SS}_{bb} = \{ii| \text{ Fare bin } (i) \in \mathcal{T}_b^* \text{ and pick-up zone } (i) \in \mathcal{Z}_b^*\} \dots\dots\dots\dots\dots\dots\dots \text{(Eq. 6)}$$

The 3SLS model is re-estimated on bootstrap sample $\mathcal{SS}_{bb}$, yielding a new set of parameter estimates $\hat{\theta\theta}_{bb}$ for that replication , producing a distribution of bootstrap estimates for each parameter. The bootstrap mean ($\theta\theta^{-}_{jj}{}^*$) and standard deviation (SD_j^*) for each parameter $\theta\theta_{jj}$ is given by

$$\theta\theta^{-*}_{j} = \frac{1}{BB}\sum_{bb=1}^{BB} \theta\theta^{\hat{}}_{bb,jj} \quad \text{and} \quad \mathrm{SD}_{jj*} = \sqrt{\frac{1}{BB-1}\sum_{bb=1}^{B}\left(\theta\hat{\theta}_{bb,jj} - \bar{\theta}^*_{jj}\right)^2}$$

RESULTS

Table 2 shows the estimated coefficients of the demand equation, all of which are statistically significant. This study further calculated practical significance, which yields a standardized measure that captures the impact of a one-standard-deviation change in a given variable on the outcome relative to the overall variability in demand. This was achieved by first generating baseline predictions using the original 3SLS model and then changing each regressor by one standard deviation while holding other variables constant. The difference between the new and baseline predicted values was computed and then standardized by dividing it by the standard deviation of the baseline predictions. The results showed that higher fares substantially reduce demand. A one-standard-deviation rise in Uber's fares is associated with a 27% reduction in demand, while the same rise in Lyft's fares leads to an 89% drop in demand. The substantially larger effect of the Lyft fare residual suggests that net variations in Lyft's pricing (beyond what is explained by Uber's fare) have a pronounced impact on passenger demand. Moreover, 1 SD longer wait times tie to a 37% reduction in demand, highlighting the strong sensitivity of consumers to delays.

Demographic factors further contribute: a one-standard-deviation increase in the number of household workers per available job in the pickup zone results in a 9% rise in demand, and denser residential areas drive a 3.6% increase in ride-hailing usage, although employment-dense zones may shift some trips to alternative modes. Several education categories showed distinct effects on ride-hailing demand. For instance, a one-standard-deviation increase in the proportion of residents with a college degree corresponds to a 31% increase in demand. In contrast, neighborhoods with a higher share of individuals holding bachelor's degrees experience a 14% decline, while those with more professional degree holders see an 11% reduction in demand. These differences likely reflect underlying disparities in income, access to alternative transportation, and preferences for convenience. Marital status influences demand as well; compared to never-married individuals, married residents exhibit approximately a 10% lower demand, whereas divorced or separated individuals and widowed individuals show modest increases of 4.4% and 3.7%, respectively.

Table 2 Demand Model Estimates (Y= $QQ^{TTTT}{}_{iiii}{}^{iiTTTT}$, N = 2194, Adj R^2 =0.613)

Variable Name	Coefficient
Passenger Wait Time (min)	-54.52
Uber's Fare ($ per mile)	-16.17
Lyft's Fare Residual (per mile)	-278.2
Gross population density (people/acre) at Pickup Zone	0.115
Gross employment density (jobs/acre) at Pickup Zone	-0.024
Count of workers earning $1250 per month or less at Pickup Zone	-0.114
Count of workers earning between $1250 to $3333 per month at Pickup Zone	0.036
Count of workers earning $3333 per month or more at Pickup Zone	0.004
Number of Jobs in Zone per Household in Pickup Zone	-0.027
Number of Household Workers per Job at Pickup Zone	2.462
College/Associate Degree Graduate people per Capita (Pickup Zone)	148.4
Bachelor's Degree Graduate people per Capita (Pickup Zone)	-363.3
Professional Degree Graduate people per Capita (Pickup Zone)	-275.4

Married (Except Separated) people per Capita (Pickup Zone)	-38.90
Divorced or Separated people per Capita (Pickup Zone)	217.2
Widowed people per Capita (Pickup Zone)	314.2
Daily Average Precipitation (mm)	-12.20
Daily Average Temperature (°C)	12.70
Daily Average wind speed (mi/h)	32.40

(All variables are statistically significant at $\alpha = 0.05$)

The fare equations reveal distinct operator-specific pricing dynamics. Uber's fare equation estimates (Table 3) indicate that real-time supply availability—approximated by wait times—has a positive and highly significant effect on per-mile charges. A one-standard-deviation rise in wait time was associated with a 9.8% rise in per-mile fares. Overall market demand, as measured by the total trip count, significantly drives fare levels: a one-standard-deviation increase in demand raises Uber's per-mile fares by 26% and Lyft's fares by 12% (Table 3 and 4), indicating that the operator's pricing algorithm responds strongly to real-time supply-demand imbalances. Demographic and economic variables also show a strong association with ride-hailing demand. zones with a higher share of top earners experience slightly lower surge levels, possibly because these areas are better serviced or see travel patterns that mitigate peak-time shortages. Meanwhile, the job concentration shows small but significant fare increases in more employment-dense areas—potentially because commuting hotspots face more frequent or pronounced surges during rush hours. Lyft's fare estimates (Table 4) show that its pricing is less sensitive to broader marketwide demand surges than to local, real-time driver availability. The share of workers in the highest wage bracket is negatively associated with fares, and the effects differ considerably among education variables. Taxi zones with a higher concentration of high school graduates tend to have elevated fares, potentially due to peak-hour usage.

In addition to the main market-level drivers, the model includes four event-based indicators that capture temporal shocks resulting from major gatherings and festivals in September 2023. The United Nations General Assembly is associated with a slight reduction in per-mile fares, whereas Climate Week and the Global Citizen Festival led to modest rises in per-mile charges. The bootstrap approach provides a comprehensive view of the variability in the 3SLS estimates across multiple resampled spatiotemporal clusters. For the demand equation, the results show moderate variability in its parameters. For instance, the initial coefficient for wait time is –54.5, with a bootstrap mean of –58.8 and a standard deviation of 44.2, indicating moderate uncertainty in its impact on demand. Lyft fare residual showed variability too, with its original coefficient at –278, a bootstrap mean of –247, and a standard deviation of 44.8. In the Uber fare equation, the impact of wait time remains relatively stable; the original coefficient of 1.14 is closely mirrored by a bootstrap mean of 1.21 and a low standard deviation of 0.12. This consistency suggests that the surge pricing effect driven by supply constraints is robust across resampled clusters. For the Lyft fare equation, similar patterns emerge. The wait time parameter is consistently estimated with an original value of 1.25 and a bootstrap mean of 1.33, with a standard deviation of 0.12, reinforcing the critical role of real-time supply in determining fare levels. Other coefficients in Lyft's fare equation, including those for demographic factors, display narrower bootstrap variances compared to some of the demand equation parameters, suggesting that Lyft's pricing is less sensitive to broader market fluctuations and more stable in response to local conditions.

Table 3 Uber's Fare Model Estimates (Y= $QQ^{TTTT}{}_{iiii}{}^{iiTTTT}$, N = 2,194, Adj R^2 =0.609)

Variable Name	Coefficient
Demand (Total Trips Requests)	0.002
Passenger Wait Time (min)	1.158
Gross employment density (jobs/acre) at Pickup Zone	9.69E-05
Count of workers earning $1250 per month or less at Pickup Zone	0.001
Count of workers earning between $1250 to $3333 per month at Pickup Zone	-0.001
Count of workers earning $3333 per month or more at Pickup Zone	-2.65E-04
High School Graduate people per Capita (Pickup Zone)	1.683
College/Associates Degree Graduate people per Capita (Pickup Zone)	-0.432
Married (Except Separated) people per Capita (Pickup Zone)	0.698
Divorced or Separated people per Capita (Pickup Zone)	2.445
Widowed people per Capita (Pickup Zone)	-0.845
UN General Assembly (September 19–23)	-1.583
Climate Week (September 17–24)	0.410
Global Citizen Festival (September 23)	0.242

(Variables are statistically significant at α = 0.05)

Table 3 Lyft's Fare Model Estimates (Y= $QQ^{TTTT}{}_{iiii}{}^{iiTTTT}$, N = 2194, Adj R^2 =0.609)

Variable Name	Coefficient
Demand (Total Trips Requests)	0.0002
Passenger Wait Time (min)	1.263
Gross employment density (jobs/acre) at Pickup Zone	-3.16E-05
Count of workers earning $1250 per month or less at Pickup Zone	0.001
Count of workers earning between $1250 to $3333 per month at Pickup Zone	-0.001
Count of workers earning $3333 per month or more at Pickup Zone	-2.87E-04
High School Graduate people per Capita (Pickup Zone)	2.566
College/Associates Degree Graduate people per Capita (Pickup Zone)	-0.409
Married (Except Separated) people per Capita (Pickup Zone)	0.884
Divorced or Separated people per Capita (Pickup Zone)	3.551
Widowed people per Capita (Pickup Zone)	-2.881
UN General Assembly Indicator (September 19–23)	-1.643
Climate Week Indicator (September 17–24)	0.078
Global Citizen Festival Indicator (September 23)	2.124

(Variables are statistically significant at α = 0.05)

CONCLUSIONS

Ride-hailing services like Uber and Lyft offer a dynamic alternative to traditional taxis and public transportation. Despite their growing significance, conventional models often overlook the feedback relationship between fare and demand across time, space, and competing providers. This study addressed this gap by jointly estimating the relationship between demand and per-mile fares for Uber and Lyft in New York City using a three-stage least squares (IV3SLS) system of simultaneous equations. On the demand side, the analysis showed that both fare levels and wait times are key drivers, with higher fares and longer wait times resulting in significantly fewer trip requests—especially for Lyft users, who showed higher sensitivity to fares compared to Uber users. A one-standard-deviation rise in Uber's fares reduces demand by 27%, whereas the same increase in Lyft's fare residual leads to an 89% drop. Longer passenger wait times, too, were associated with a 37% reduction in demand, emphasizing that riders are highly sensitive to delays. These associations are additionally affected by underlying demographic and environmental conditions. The results showed that educational attainment and income levels have a differentiated impact on ride-hailing demand—areas with more college-educated residents show a 31% increase in demand, while regions with higher proportions of bachelor's or professional degree holders experience declines.

Marital status also plays a role, with married individuals showing lower demand relative to nevermarried individuals, while divorced or widowed populations exhibit modest increases. Weather conditions are equally influential; rainy conditions reduce demand by 17%, whereas hotter temperatures and higher wind speeds lead to modest increases, reflecting consumers' preferences for comfort and convenience. On the fare side, both Uber and Lyft employ dynamic pricing models that respond to real-time supply constraints. The results showed that fares increased with longer wait times, reflecting the surge pricing effect triggered by limited driver availability. However, Uber's fares were observed to be more responsive to overall market demand than those of Lyft. One standard deviation increase in total trip count leads to a 26% increase in Uber's fares and a 12% increase in Lyft's fares. Moreover, wealthier neighborhoods tend to experience lower surge levels, likely due to higher driver availability or less pronounced peak-hour fluctuations. In contrast, middle- and lower-income areas tend to see slightly higher fares, suggesting greater supply-demand mismatches in these regions. External conditions, such as, weather, are equally influential; rainy conditions reduce demand by 17%, whereas hotter temperatures and higher wind speeds lead to modest increases, reflecting consumers' preferences for comfort and convenience. The bootstrap results further illuminated the role of spatiotemporal dependencies in the ridehailing market.

Although the demand estimates show only moderate variability across clusters, this moderate variability reflects meaningful local and temporal heterogeneity that significantly influences consumer behavior. For example, the effect of wait time on demand differs considerably across taxi zones and time intervals, suggesting that localized congestion and regional economic conditions have a substantial impact on ride-hailing usage. In contrast, the fare equations for both Uber and Lyft display remarkably stable wait time coefficients. This stability implies that surge pricing mechanisms are robust across diverse spatiotemporal clusters—regardless of the specific pickup zone or time of day, the response to supply constraints remains consistent.

These outcomes emphasize the diverse factors influencing ride-hailing dynamics, which are systematically examined by addressing several key challenges simultaneously. It resolves simultaneity by modeling the bidirectional feedback between operator-specific fares and demand using instruments within a three-stage least squares framework. It captures spatiotemporal dependencies by including both within-cluster and cross-cluster correlations across time and space, revealing distinct pricing strategies and demand sensitivities across competitors. Future research should extend the timeframe to capture longer-term and seasonal variations, particularly under evolving regulatory regimes like new tolling policies. Further exploration into different service tiers, namely, premium or luxury options, and a deeper examination of driver-side factors—including acceptance rates and fleet size—are warranted. Exploring unobserved rider factors, like brand loyalty and past wait-time experiences, may further refine the understanding of operator preferences and lead to more adaptive fare strategy models.

ACKNOWLEDGMENTS

This article and the work described were sponsored by the U.S. Department of Energy (DOE) Vehicle Technologies Office (VTO) under the Systems and Modeling for Accelerated Research in Transportation (SMART) Mobility Laboratory Consortium, an initiative of the Energy Efficient Mobility Systems (EEMS) Program. The U.S. Government retains for itself, and others acting on its behalf, a paid-up nonexclusive, irrevocable worldwide license in said article to reproduce, prepare derivative works, distribute copies to the public, and perform publicly and display publicly, by or on behalf of the Government.

AUTHOR CONTRIBUTIONS

The authors confirm the contribution to the paper as follows: Conceptualization, data curation, formal analysis, investigation and methodology: Priyanka, P.; Gurumurthy, K.M; and Kockelman, K.; Project administration and Supervision: Kockelman, K. and Gurumurthy, K.M; Visualization and Writing – original draft: Priyanka, P., Kockelman, K.; Writing – review & editing: Kockelman, K. and Gurumurthy, K.M; The authors confirm their respective contributions to this manuscript as outlined above. We acknowledge and thank Aditi Bhasker for her review and valuable feedback.

REFERENCES

Chao, J., 2019. Modeling and Analysis of Uber’s Rider Pricing. Proceedings of the International Conference on Economic Management and Cultural Industry (ICEMCI 2019), Atlantis Press, pp. 693–711.

Chen, C., Feng, T., Ding, C., Yu, B. and Yao, B., 2021. Examining the spatial-temporal relationship between urban built environment and taxi ridership: Results of a semiparametric GWPR model. Journal of Transport Geography, 96, p.103172.

Chen, Q., Lei, Y. and Jasin, S., 2023. Real-Time Spatial–Intertemporal Pricing and Relocation in a Ride-Hailing Network: Near-Optimal Policies and the Value of Dynamic Pricing. Operations Research. https://doi.org/10.1287/opre.2022.2425.

Chen, X.M., Zheng, H., Ke, J. and Yang, H., 2020. Dynamic Optimization Strategies for OnDemand Ride Services Platform: Surge Pricing, Commission Rate, and Incentives. Transportation Research Part B: Methodological, 138, pp.23–45.

City of New York, 2024. Congestion Pricing Program. Available at: https://portal.311.nyc.gov/article/?kanumber=KA-03612 [Accessed 25 March 2025].

Correa, D., 2017. Exploring the taxi and Uber demands in New York City: An empirical analysis and spatial modeling. SSRN 4229042.

Dey, B.K., Tirtha, S.D., Eluru, N. and Konduri, K.C., 2021. Transformation of Ride-Hailing in New York City: A Quantitative Assessment. Transportation Research Part C: Emerging Technologies, 129, p.103235.

Feng, Y., Niazadeh, R. and Saberi, A., 2024. Two-Stage Stochastic Matching and Pricing with Applications to Ride Hailing. Operations Research, 72(4), pp.1574–1594. https://doi.org/10.1287/opre.2022.2398.

Gurumurthy, K.M., Kockelman, K.M. and Auld, J., 2021. A system of shared autonomous vehicles for Chicago. Journal of Transport and Land Use, 14(1), pp.933–948.

He, S. and Shin, K.G., 2019. Spatio-temporal Adaptive Pricing for Balancing Mobility-onDemand Networks. ACM Transactions on Intelligent Systems and Technology, 10(4), Article 39. https://doi.org/10.1145/3331450.

Huang, G., Liang, Y. and Zhao, Z., 2023. Understanding Market Competition Between Transportation Network Companies Using Big Data. Transportation Research Part A: Policy and Practice, 178, p.103861.

Huang, H., 2023. Taxi Fare Prediction Based on Multiple Machine Learning Models. Proceedings of the 5th International Conference on Computing and Data Science. doi: 10.54254/2755-2721/16/20230849.

Jäger, B., Wittmann, M. and Lienkamp, M., 2016. Analyzing and modeling a City's spatiotemporal taxi supply and demand: A case study for Munich. Journal of Traffic and Logistics Engineering, 4(2).

Ke, J., Zheng, H., Yang, H. and Chen, X., 2020. Pricing Strategies for Ride-Sourcing Platforms: A Dynamic Game-Theoretic Approach. Transportation Research Part C: Emerging Technologies, 113, pp.73–92.

Kelleny, B. and Ishak, S., 2021. Exploring and visualizing spatial effects and patterns in ridesourcing trip demand and characteristics. Journal of Sustainable Development of Transport and Logistics, 6(2), pp.6–24. https://doi.org/10.14254/jsdtl.2021.6-2.1.

Lavieri, P.S., Dias, F.F., Juri, N.R., Kuhr, J. and Bhat, C.R., 2018. A model of ridesourcing demand generation and distribution. Transportation Research Record, 2672(46), pp.31–40.

Li, B., Cai, Z., Jiang, L., Su, S. and Huang, X., 2019. Exploring urban taxi ridership and local associated factors using GPS data and geographically weighted regression. Cities, 87, pp.68–86.

Liu, X., Gong, L., Gong, Y. and Liu, Y., 2015. Revealing travel patterns and city structure with taxi trip data. Journal of Transport Geography, 43, pp.78–90.

Liu, Y., Wang, F., Xiao, Y. and Gao, S., 2012. Urban land uses and traffic ‘source-sink areas’: Evidence from GPS-enabled taxi data in Shanghai. Landscape and Urban Planning, 106(1), pp.73–87.

Lyft Blog, 2025. Navigating the New NYC Congestion Fee with Lyft. Available at: https://www.lyft.com/blog/posts/navigating-the-new-nyc-congestion-fee-with-lyft [Accessed 2 February 2025].

McNally, M.G. and Rafiq, R., 2021. Analysis of Activity-Travel Patterns and Tour Formation of Transit Users. Pacific Southwest Region University Transportation Center, Report No. PSR-19-33.

Meskar, M., Aslani, S. and Modarres, M., 2023. Spatio-temporal pricing algorithm for ridehailing platforms where drivers can decline ride requests. Transportation Research Part C: Emerging Technologies, 153, p.104200.

Meteostat, 2023. Meteostat Python library. GitHub. Available at: https://github.com/meteostat/meteostat [Accessed 25 March 2025].

Moreira-Matias, L., Gama, J., Ferreira, M., Mendes-Moreira, J. and Damas, L., 2013. Predicting taxi–passenger demand using streaming data. IEEE Transactions on Intelligent Transportation Systems, 14(3), pp.1393–1402.

New York City Taxi and Limousine Commission (2024) *2024* Annual Report. Available at: https://www.nyc.gov/assets/tlc/downloads/pdf/annual_report_2024.pdf (Accessed: 2725 April 2025).

New York City Taxi and Limousine Commission, 2024. Industry Notice #24-10: MTA Congestion Pricing Toll to Go into Effect January 5, 2025. Available at: https://www.nyc.gov/assets/tlc/downloads/pdf/industrynotices/industry_notice_24_10_english.pdf [Accessed 25 March 2025].

New York City Taxi and Limousine Commission, 2025. TLC Trip Record Data. Available at: https://www.nyc.gov/site/tlc/about/tlc-trip-record-data.page [Accessed 25 March 2025].

New York State Department of Taxation and Finance, 2024. Congestion Surcharge. Available at: https://www.tax.ny.gov/bus/cs/csidx.htm [Accessed 25 March 2025].

Oh, S., Kondor, D., Seshadri, R., Zhou, M., Le, D.-T. and Ben-Akiva, M., 2020. Spatiotemporal Characteristics of Ride-sourcing Operation in Urban Area. Available at: http://export.arxiv.org/pdf/2011.07673 [Accessed 25 March 2025].

Özkan, E., 2020. Joint pricing and matching in ride-sharing systems. European Journal of Operational Research, 287(3), pp.1149–1160.

Paithankar, P., Fakhrmoosavi, F., Kockelman, K.M. and Perrine, K.A., 2024. International Travel Patterns: Exploring Destination Preferences and Airfare Trends to and from the USA. Transportation Planning and Technology, pp.1–19.

Pan, R., Zhang, S., Yang, H., Xie, K. and Wen, Y., 2019. Analysis of spatial equity in taxi services: A case study of New York City. In 2019 IEEE Intelligent Transportation Systems Conference (ITSC), IEEE, pp.2659–2664.

Paronda, A.G.A., Regidor, J.R.F. and Napalang, M.S.G., 2016. Comparative Analysis of Transportation Network Companies (TNCs) and Conventional Taxi Services in Metro Manila. Proceedings of the 23rd Annual Conference of the Transportation Science Society of the Philippines, Vol. 8.

Parvez, D.A., Tirtha, S.D., Bhowmik, T. and Eluru, N., 2023. Joint Econometric Model Framework for Transportation Network Company Users' Trip Fare and Destination Choice Analysis. Transportation Research Record: Journal of the Transportation Research Board, 2677(7), pp.545–557.

Qian, X. and Ukkusuri, S.V., 2015. Spatial variation of the urban taxi ridership using GPS data. Applied Geography, 59, pp.31–42.

Schwieterman, J.P., 2019. Uber economics: Evaluating the monetary and travel time trade-offs of transportation network companies and transit service in Chicago, Illinois. Transportation Research Record, 2673(4), pp.295–304.

Tang, J., Gao, F., Liu, F., Zhang, W. and Qi, Y., 2019. Understanding Spatio-Temporal Characteristics of Urban Travel Demand Based on the Combination of GWR and GLM. Sustainability, 11(19), p.5525. https://doi.org/10.3390/su11195525.

US Department of Transportation (2016) Revised Departmental Guidance on Valuation of Travel Time in Economic Analysis. Washington, DC: US Department of Transportation. https://www.dot.gov/sites/dot.gov/files/docs/2016%20Revised%20Value%20of%20Travel%20Time%20Guidance.pdf (Accessed: 25 April 2025).

Wang, H. and Yang, H., 2019. Ridesourcing systems: A framework and review. Transportation Research Part B: Methodological, 129, pp.122–155.

Wang, X., He, F., Yang, H. and Gao, H.O., 2016. Pricing Strategies for a Taxi-Hailing Platform. Transportation Research Part E: Logistics and Transportation Review, 93, pp.212– 231.

Xing, D., Zhao, C. and Wang, G., 2022. A Spatial-Temporal Attention Multi-Graph Convolution Network for Ride-Hailing Demand Prediction Based on Periodicity with Offset. arXiv preprint arXiv:2203.12505. https://doi.org/10.48550/arXiv.2203.12505.

Yu, H. and Peng, Z.R., 2020. The impacts of built environment on ridesourcing demand: A neighbourhood level analysis in Austin, Texas. Urban Studies, 57(1), pp.152–175.

Zha, L., Yin, Y. and Du, Y., 2017. Surge Pricing and Labor Supply in the Ride-Sourcing Market. Transportation Research Procedia, 23, pp.2–21. https://doi.org/10.1016/j.trpro.2017.05.002.

Zhang, D., Xiao, F., Kou, G., Luo, J. and Yang, F., 2023. Learning Spatial-Temporal Features of Ride-Hailing Services with Fusion Convolutional Networks. Journal of Advanced Transportation, 2023, pp.1–12. https://doi.org/10.1155/2023/4427638.

Zhao, K., Khryashchev, D., Freire, J., Silva, C. and Vo, H., 2016. Predicting taxi demand at high spatial resolution: Approaching the limit of predictability. In 2016 IEEE International Conference on Big Data (Big Data), IEEE, pp.833–842.

Zheng, Z., Zhang, J., Zhang, L., Li, M., Rong, P. and Qin, Y., 2022. Understanding the impact of the built environment on ride-hailing from a spatio-temporal perspective: A fine-scale empirical study from China. Cities, 126, p.103706. https://doi.org/10.1016/j.cities.2022.103706.

Zhou, X., Wang, M. and Li, D., 2019. Bike-sharing or taxi? Modeling the choices of travel mode in Chicago using machine learning. Journal of Transport Geography, 79, p.102479.

Zhou, Y., Yang, H. and Ke, J., 2022. Price of Competition and Fragmentation in Ride-Sourcing Markets. Transportation Research Part C: Emerging Technologies, 143, p.103851.

Zhou, Y., Yang, H., Ke, J., Wang, H. and Li, X., 2022. Competition and Third-Party PlatformIntegration in Ride-Sourcing Markets. Transportation Research Part B: Methodological, 159, pp.76–103.

Zhu, P. and Mo, H., 2022. The potential of ride-pooling in VKT reduction and its environmental implications. Transportation Research Part D: Transport and Environment, 103, p.103155.

Zhu, P., Huang, J., Wang, J., Liu, Y., Li, J., Wang, M. and Qiang, W., 2022. Understanding taxi ridership with spatial spillover effects and temporal dynamics. Cities, 125, p.103637. https://doi.org/10.1016/j.cities.2022.103637.